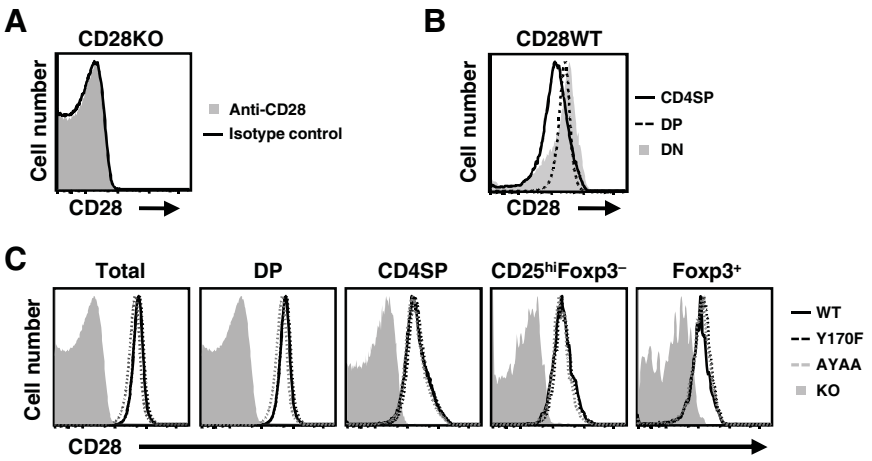

Figure S1. Surface expression of CD28. (A) Validation of CD28 staining. Total thymocytes from CD28 KO mice were stained with either anti-CD28 (shaded) or isotype control (solid line) and analyzed by flow cytometry. (B) Expression of CD28 is inversely correlated with thymocyte maturation. CD28 expression on the indicated thymic subsets from WT mice was analyzed. DN, HSA^{hi} $CD4^{-}CD8^{-}$ double negative (shaded); DP, $CD4^{+}CD8^{+}$ double positive (dashed line); CD4SP, $CD4^{+}CD8^{-}$ single positive (solid line). (C) CD28 knockin mice express WT level of CD28. CD28 expression on indicated thymocyte subsets from WT, CD28–Y170F, AYAA, and KO were analyzed by flow cytometry. Data are representative of at least five independent experiments.

Figure S1

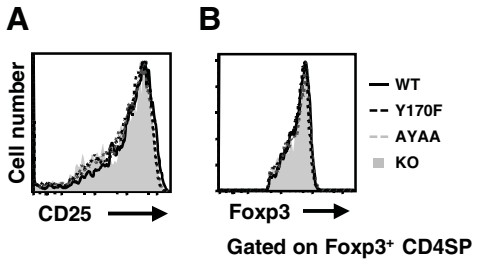

Figure S2. Normal expression of CD25 and Foxp3 by Treg cells from CD28 mutant and KO mice. Expression of CD25 and Foxp3 was analyzed by flow cytometry. Plots are gated on the Foxp3$^+$ CD4SP subset.

Figure S2

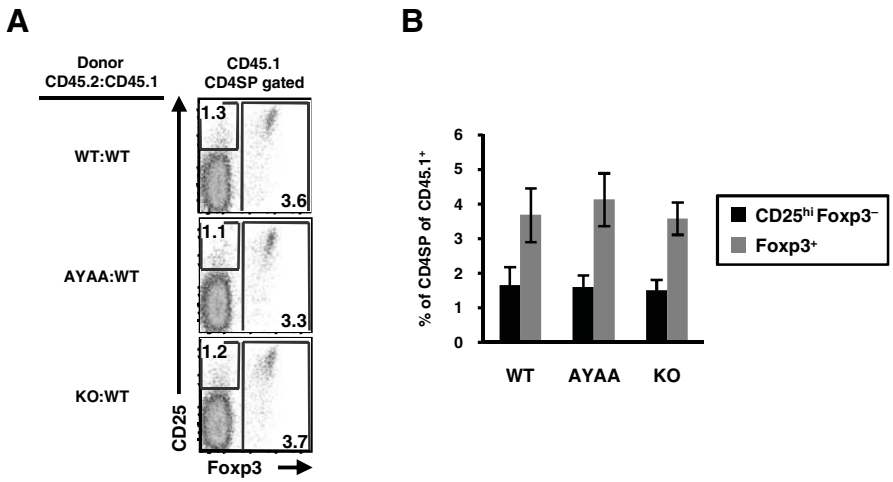

Figure S3. The overall environment for Treg cell development in mixed bone marrow chimeras appears normal. (A) Lethally irradiated congenic hosts (CD45.1) were reconstituted with an equal mixture of bone marrow cells from Foxp3^{gfp} WT (CD45.1) and WT, KO, or AYAA (all CD45.2) mice as per Fig. 2B. Foxp3 and CD25 expression in CD45.1^{+}CD4SP cells were analyzed by flow cytometry six weeks post-reconstitution. (B) The average percentage of CD25^{hi}Foxp3^{-} and Foxp3^{+} cells (+/- S.D.) within the CD45.1^{+}CD4SP subset are summarized (n=8 for WT, AYAA, and KO). The number of mice analyzed is slightly different from Fig. 2B as CD45.1 *Foxp3*^{WT} and not *Foxp3*^{gfp} mice were used in some mixed bone marrow chimera experiments.

Figure S3

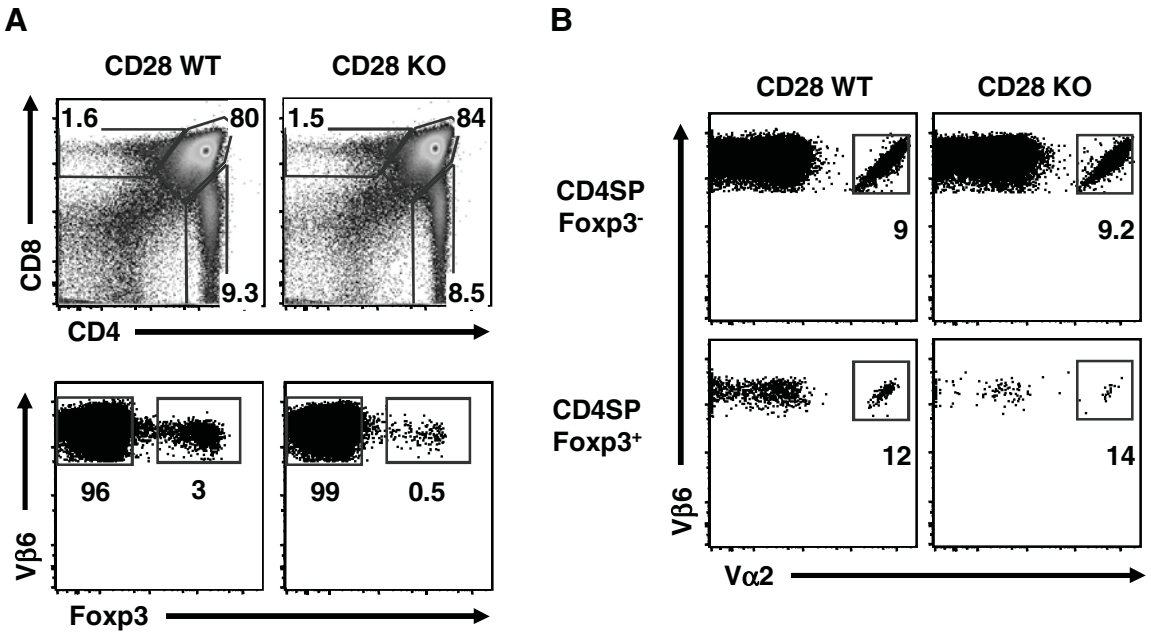

Figure S4. Thymic development in TCliβ-tg CD28 KO mice. (A) Thymocytes from CD28 WT and KO TCliβ-tg *Foxp3*^{gfp} *Tcra*$^{+/-}$ mice were analyzed by flow cytometry for CD4 and CD8 (top), and Foxp3 expression on Vβ6^{+} cells (bottom). The TCliβ chain is Vβ6. (B) The percentage of Vα2^{+} cells within the Foxp3^{-} and Foxp3^{+} CD4SP subsets is shown. Plots are gated on Vβ6^{+} cells.

Figure S4

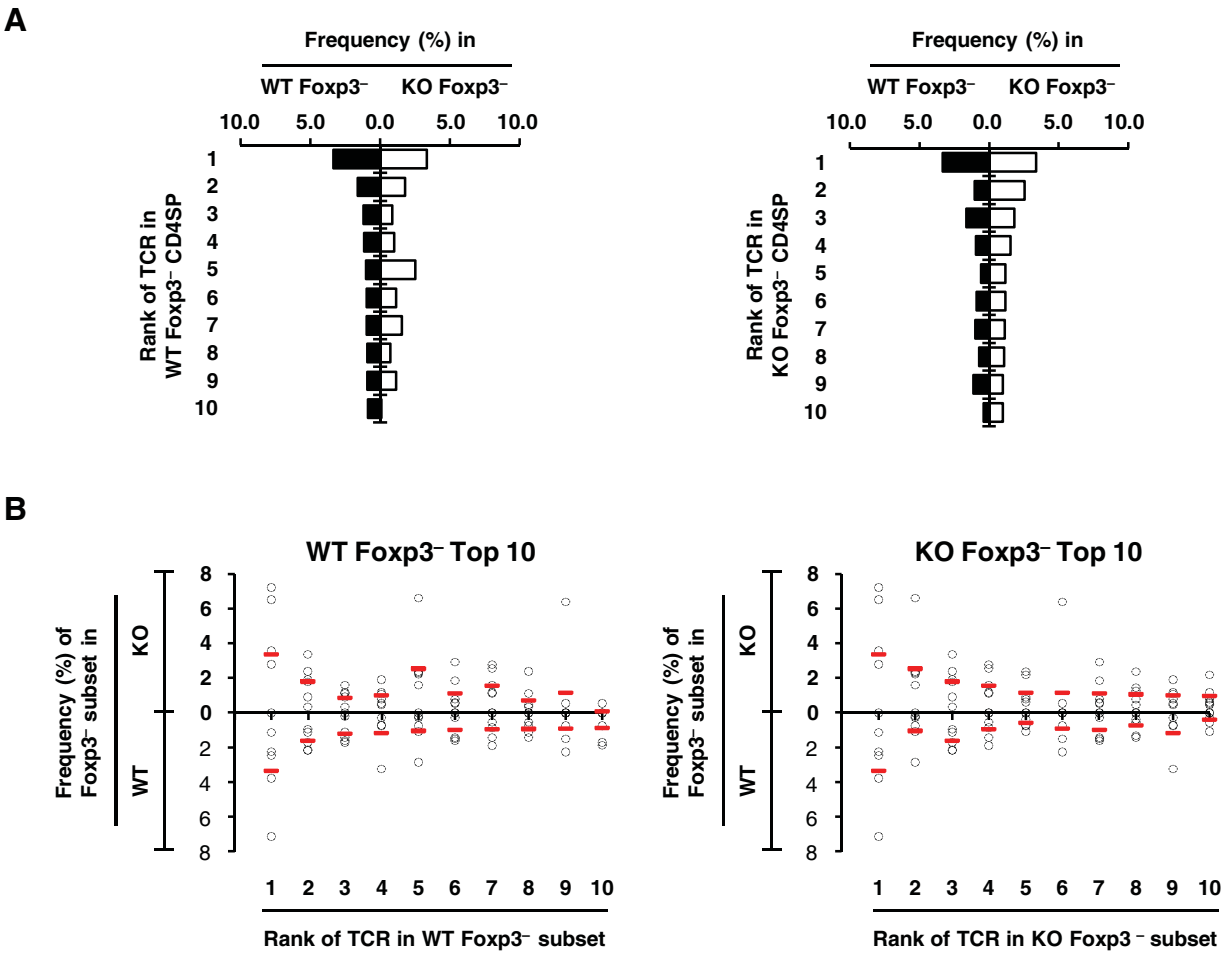

Figure S5. The TCR repertoires of Foxp3⁻ cells from CD28 WT and KO are largely overlapping. (A) The top 10 TCRs in the Foxp3⁻ CD4SP data sets from CD28 WT (left) or KO (right) mice are shown. The frequency of the TCR in the CD28 WT and KO Foxp3⁻ CD4SP data sets is shown. (B) The frequency of the Top 10 TCRs within the individual data sets is shown. Each dot represents an individual data set, and the bars indicate the average frequency.

Figure S5

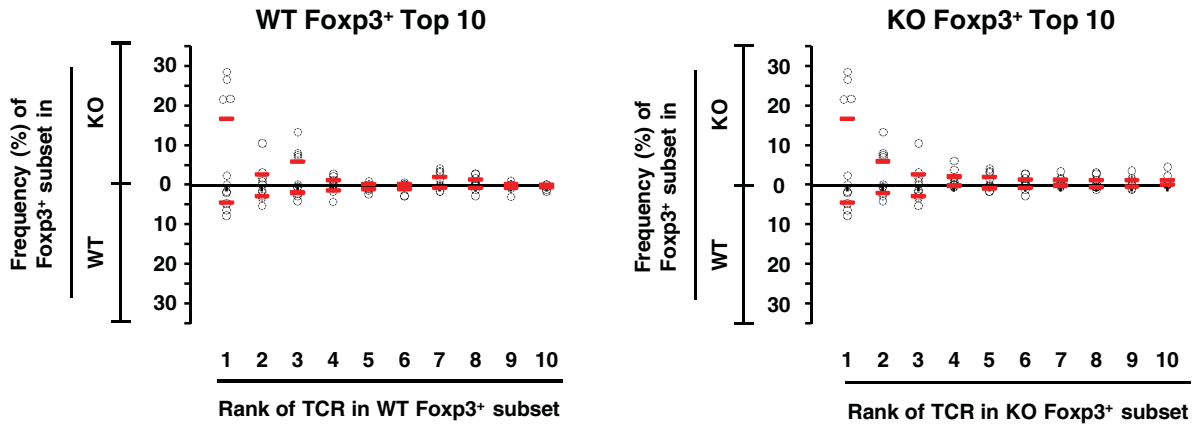

Figure S6. Frequency of top 10 Foxp3⁺ TCRs in individual data sets. The frequency of the top 10 TCRs from individual datasets of CD28 WT (left) and KO (right) is shown. Bars indicate the average frequency.

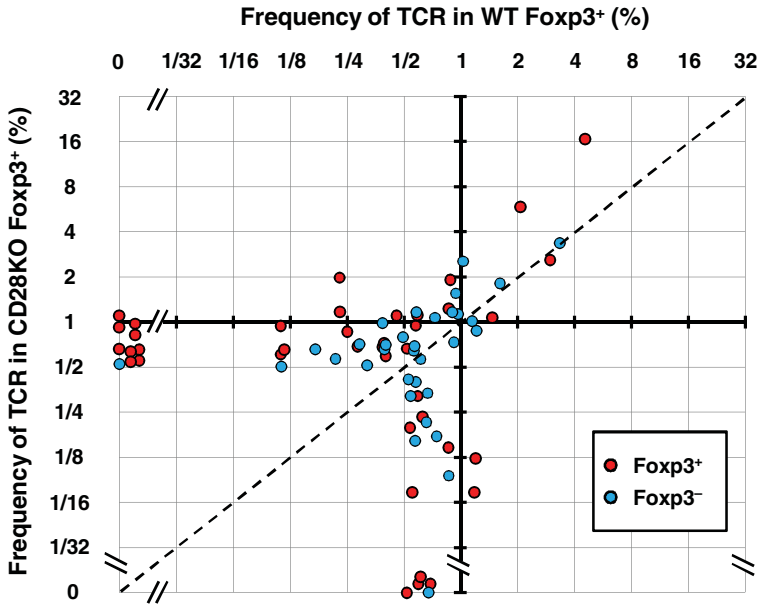

Figure S7. Two dimensional plot of TCRs above 0.5% frequency in either the CD28 KO or WT data sets. Data was plotted as in Figure 5. Forty and thirty-three TCRs are shown for Foxp3⁺ and Foxp3⁻ data sets. About 25.4% and 50.3% of total TCR is shown for WT and KO Foxp3⁺ and 23.8 %and 27.0% for WT and KO⁻ data sets. Of note, four and nine TCRs are unique to those found in WT and KO Foxp3⁺ subsets, whereas only one TCR is unique to WT and KO Foxp3⁻ subsets.

Figure S6 and S7

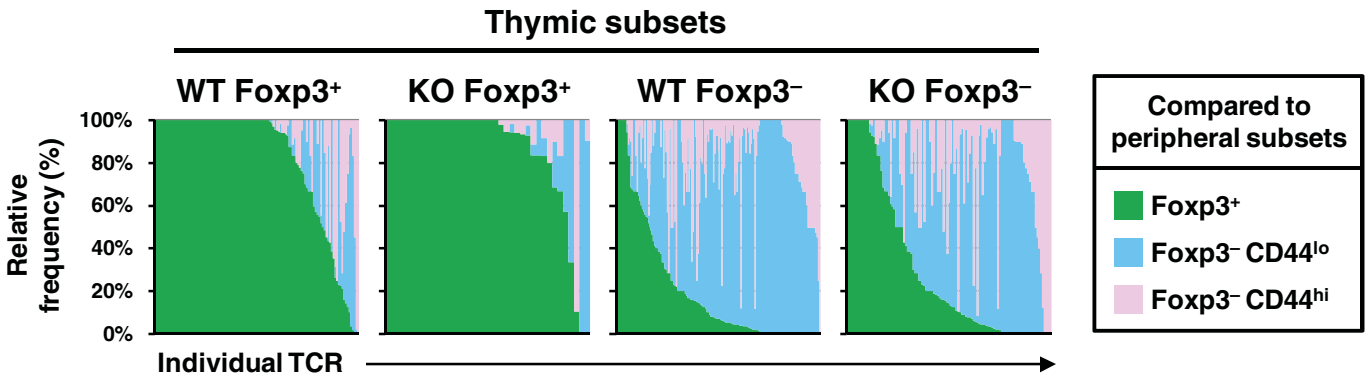

Figure S8. Comparison of CD28 WT or KO thymic TCRs to peripheral WT TCRs data sets. TCRs from thymic Foxp3$^+$ and Foxp3$^-$ CD4SP subsets in CD28 WT and KO mice were compared to previously described peripheral TCR datasets (Lio and Hsieh, *Immunity* 28:100, 2008). Only TCRs that are found in more than one data set from the indicated thymic subsets were analyzed (Table S1). Among those TCRs, 116/132 (87.9%), 38/45 (84.4%), 161/168 (95.8), and 110/125 (88.0%) TCRs from thymic CD28 WT Foxp3$^+$, KO Foxp3$^+$, WT Foxp3$^-$, and KO Foxp3$^-$ CD4SP subsets, respectively, were found in the peripheral TCR datasets and included in the graphs. The peripheral TCR data sets contain ~18,000 total sequences from Foxp3$^+$, Foxp3$^-$CD44^{lo}, Foxp3$^-$CD44^{hi} cells isolated from the spleen; and inguinal, auxiliary, cervical, and mesenteric lymph nodes. The relative frequency of individual TCRs that are found in the peripheral Foxp3$^+$ (green), CD44^{lo} (blue), and CD44^{hi} (pink) subsets are depicted by the height of the bar. For example, a thymic TCR that is exclusively found in peripheral Treg cells would be shown as a green bar; whereas a TCR that is equally found in Foxp3$^-$ CD44^{lo} and CD44^{hi} subsets would be shown as a half blue and half pink bar. As the thymic CD28 KO Treg repertoire is somewhat smaller and shifted in comparison with the WT Treg repertoire (Table S1, Fig. 5), the number of thymic TCRs found in the normal peripheral data sets is lower. With that caveat in mind, we do observe a trend suggesting that thymic CD28 KO Treg cells use TCRs which are more efficient at generating Treg cells in WT mice. Conversely, the thymic CD28 KO Foxp3$^-$ repertoire contains more TCRs which are found in peripheral Treg cells in WT mice. Taken together, these data show a trend suggesting that CD28 plays a role in assisting TCRs that are inefficient at inducing Treg cell development. Note that this analysis does not incorporate the frequency of the TCR in the population. However, other analyses (Fig. 5) suggests that the actual number of cells expressing CD28-dependent Treg TCRs is relatively small.

Figure S8

	CD28 WT		CD28 KO	
	Foxp3$^+$	**Foxp3$^-$**	**Foxp3$^+$**	**Foxp3$^-$**
Number of data sets	5	5	6	6
Total number of sequences	1305	1474	1090	1109
Unique TCRs	677	886	371	622
% of Total from Top 10 TCRs	16.7	13.0	34.8	15.8
% of Total from Top 20 TCRs	22.5	19.4	43.5	22.8
ACE	577.7	767.0	166.2	751.5

Table S1. Summary of TRAV14 (Vα2) sequences obtained from CD28 KO and WT TCli TCRβ transgenic mice. TRAV14 TCR sequences from Foxp3$^+$ and Foxp3$^-$ CD4SP thymocytes were obtained as previously described (7). Each CD28 KO data set is from an individual mouse. The WT data sets include 2 from individual mice and 3 from pools of several mice previously described (16). Each data set is comprised of approximately 200 sequences. The total number of sequences from all of the data sets, and the total number of unique TCRs assessed using the CDR3 amino acid sequence, are shown. The fractional composition of the 10 or 20 most frequent TCRs within the combined data sets, and the abundance coverage estimator (ACE), are shown as indicators of oligoclonality within the TCR repertoire.

Table S1